

DoD Stabilization of linear hyperbolic PDEs on general cut-cell meshes

Gunnar Birke^{1,*}, Christian Engwer¹, Sandra May², and Florian Streitbürger³.

¹ Applied Mathematics Münster, Münster University

² Department of Information Technology, Uppsala University

³ Department of Mathematics, Dortmund University

Standard numerical methods for hyperbolic PDEs require for stability a CFL-condition which implies that the time step size depends on the size of the elements of the mesh. On cut-cell meshes, elements can become arbitrarily small and thus the time step size cannot take the size of small cut-cells into account but has to be chosen based on the background mesh elements.

A remedy for this is the so called DoD (domain of dependence) stabilization for which several favorable theoretical and numerical properties have been shown in one and two space dimensions [4, 9]. Up to now the method is restricted to stabilization of cut-cells with exactly one inflow and one outflow face, i.e. triangular cut-cells with a no-flow face (see [4]).

We extend the DoD stabilization to cut-cells with multiple in- and outflow faces by properly considering the flow distribution inside the cut-cell. We further prove L^2 -stability for the semi-discrete formulation in space and present numerical results to validate the proposed extension.

Copyright line will be provided by the publisher

1 Introduction

To avoid the mesh generation process of complex geometries, cut-cell methods are an attractive alternative. The general idea is to start with a simple, e.g. structured, background mesh and to cut out the desired geometry. This results in a mesh with unstructured polyhedral cells, called cut-cells. Cut-cells can have an arbitrary shape and can become arbitrarily small, causing the small cell problem. To use explicit time stepping schemes for solving hyperbolic conservation laws, the time step size would need to be chosen based on the smallest cut-cell in the grid to ensure stability, which is in general not feasible.

Developing solution approaches to the small cell problem in the context of discontinuous Galerkin (DG) schemes is a very recent research branch, including for example the work in [7, 8, 10]. In this contribution we focus on the domain of dependence (DoD) stabilization, which was introduced in [4] for the linear transport equation in one and two space dimensions and was extended to non-linear systems in one space dimension in [9]. It is based on a DG scheme in space to allow for higher-order approximations and possesses several desirable theoretical properties. Numerical results show the expected higher-order behavior in smooth flow and robustness around shocks.

Up to now, the DoD stabilization in two dimensions has only been used to stabilize small triangular cut-cells for linear advection parallel to a ramp [4, 11]. In this setup, the small stabilized cut-cells have exactly one inflow and one outflow face, which was exploited in the design of the stabilization. When moving to non-linear or coupled linear problems, this does not hold true anymore and one has to deal with multiple inflow and outflow faces.

In this work, we take the first step in that direction by considering the linear advection equation on a cut-cell mesh with arbitrary flow directions, resulting in triangular cut-cells having 2 inflow and 1 outflow neighbor or reverse. As this causes significant additional complications, we will only consider piecewise constant polynomials here. We will prove L^2 -stability for the semi-discrete scheme and present numerical results to validate the new extension of the stabilization terms.

The outline of the paper is as follows: we will first describe the problem setup and then introduce the new extended stabilization. Then we will show the L^2 -stability proof and conclude with numerical results.

2 Problem setup

Let $\Omega \subset \mathbb{R}^2$ be an open and connected domain. We consider linear hyperbolic systems of the form

$$u_t + Au_x + Bu_y = 0 \quad \text{in } \Omega \times (0, T), \quad (1a)$$

$$\tau u = g \quad \text{on } \partial\Omega \times (0, T), \quad (1b)$$

$$u = u_0 \quad \text{on } \Omega \times \{t = 0\}, \quad (1c)$$

where $u(t) \in \mathbb{R}^m$, and $A, B \in \mathbb{R}^{m \times m}$ constant, and τ is an appropriate boundary operator such that we only impose inflow boundary conditions on incoming waves (and not everywhere on $\partial\Omega$). We require that for any unit vector $n = (n_1, n_2)^T \in \mathbb{S}^1$ the matrices $C = (n_1 A + n_2 B)$ are symmetric and simultaneously diagonalizable over the reals, i.e. there is an orthogonal matrix $O \in \mathbb{R}^{m \times m}$ and diagonal matrices $\Lambda_n \in \text{Diag}(\mathbb{R}^{m \times m})$ such that $n_1 A + n_2 B = O \Lambda_n O^T \forall n \in \mathbb{S}^1$.

* Corresponding author: e-mail g_birk01@wwu.de

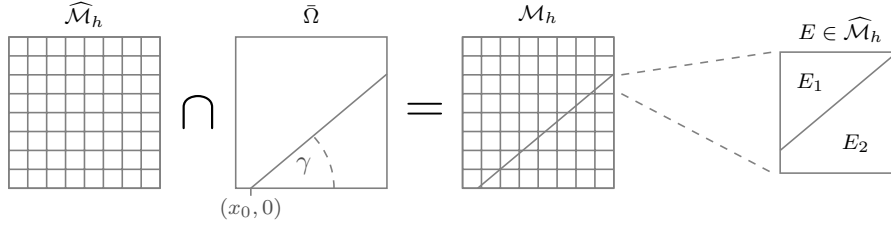


Fig. 1: Construction of the mesh: Out of the structured grid $\widehat{\mathcal{M}}_h$ on the domain Ω the mesh \mathcal{M}_h is constructed by introducing cut-cells $E_1, E_2 \subset E \in \widehat{\mathcal{M}}_h$ along the cut such that $\bar{E}_1 \cup \bar{E}_2 = \bar{E}$.

In our numerical tests we will choose $\Omega = [0, 1]^2$ and discretize it by a structured grid $\widehat{\mathcal{M}}_h$. We then introduce an artificial cut, a straight line going through the square, starting at $(x_0, 0)$ and having an angle γ relative to the x -axis. This creates an internal boundary with two subdomains which we will resolve by a cut-cell mesh \mathcal{M}_h . A sketch is contained in Fig. 1. So far we have always tested with flow parallel to that cut. Here, we consider flow in various directions, keeping the cut fixed.

We define the sets of internal and external faces as

$$\mathcal{F}_h^{\text{int}} = \{F = \partial E_1 \cap \partial E_2 \mid E_1, E_2 \in \mathcal{M}_h, E_1 \neq E_2, |F| > 0\}, \quad \mathcal{F}_h^{\text{ext}} = \{F = \partial E \cap \partial \Omega \mid E \in \mathcal{M}_h, |F| > 0\},$$

and the set of faces of an element $E \in \mathcal{M}_h$ by $\mathcal{F}_h^E = \{F \in \mathcal{F}_h^{\text{int}} \cup \mathcal{F}_h^{\text{ext}} \mid F \subset \partial E\}$. We choose a fixed local numbering on each of these sets and denote the neighbor element of E corresponding to a face $F_i \in \mathcal{F}_h^E$ by E_i . For the discretization in space we choose the discrete function space

$$\mathcal{V}_h^0(\mathcal{M}_h) = \{v_h \in L^2(\Omega)^m \mid (v_h)_i|_E \in \mathcal{P}^0(E) \forall (E, i) \in \mathcal{M}_h \times \{1, \dots, m\}\}.$$

For $v_h \in \mathcal{V}_h^0(\mathcal{M}_h)$ we denote by v_h^E the value of v_h on an element $E \in \mathcal{M}_h$.

For interior faces $F \in \mathcal{F}_h^{\text{int}}$ we fix an orientation of the outer unit normal vector n_F and denote the inner and outer element of F by E_1 and E_2 , respectively. We then define average and jump by

$$\{\{u_h\}\} := \frac{1}{2}(u_h^{E_1} + u_h^{E_2}), \quad \llbracket u_h \rrbracket := u_h^{E_1} - u_h^{E_2}.$$

For exterior faces $F \in \mathcal{F}_h^{\text{ext}}$ we simply choose the unit outer normal and denote by $u_h^{E_F}$ the solution on the cell that lies in the interior of the domain and contains face F . We define the flux matrix on a face F as

$$C_F = (n_F)_1 A + (n_F)_2 B = O \Lambda_F O^T, \quad (2)$$

where $(n_F)_{1,2}$ denote the first and second component of the unit normal vector n_F on face F . Based on this, we define matrices which encode the flux directions as

$$C_F^+ = O \Lambda_F^+ O^T, \quad C_F^- = O \Lambda_F^- O^T \quad \text{with} \quad (\Lambda_F^+)_{i,i} = \max(0, (\Lambda_F)_{i,i}) \quad \text{and} \quad (\Lambda_F^-)_{i,i} = \min(0, (\Lambda_F)_{i,i}).$$

Note that $C_F = C_F^+ + C_F^-$. We also introduce a generalization of the absolute value for such flux matrices by $|C_F| = C_F^+ - C_F^-$.

The (unstabilized) upwind semi-discretization in space is then given as: Find $u_h(t) \in \mathcal{V}_h^0(\mathcal{M}_h)$ such that

$$(\partial_t u_h(t), v_h)_{L^2(\Omega)} + a_h^{\text{upw}}(u_h(t), v_h) + l_h(v_h) = 0 \quad \forall v_h \in \mathcal{V}_h^0(\mathcal{M}_h) \quad (3)$$

with

$$a_h^{\text{upw}}(u_h, v_h) = \sum_{F \in \mathcal{F}_h^{\text{ext}}} \int_F \langle C_F^+ u_h^{E_F}, v_h^{E_F} \rangle ds + \sum_{F \in \mathcal{F}_h^{\text{int}}} \int_F \langle C_F \{\{u_h\}\}, \llbracket v_h \rrbracket \rangle + \frac{1}{2} \langle |C_F| \llbracket u_h \rrbracket, \llbracket v_h \rrbracket \rangle ds,$$

$$l_h(v_h) = - \sum_{F \in \mathcal{F}_h^{\text{ext}}} \int_F \langle C_F^- g, v_h^{E_F} \rangle ds.$$

Here, $\langle \cdot, \cdot \rangle$ denotes the scalar product in \mathbb{R}^m . We obtain a_h^{upw} and l_h by integration by parts, where the integral over internal edges leads to jump terms (second sum) and the boundary integral is split into outgoing waves (first sum) and incoming waves (right hand side). We then discretize in time using the explicit Euler scheme.

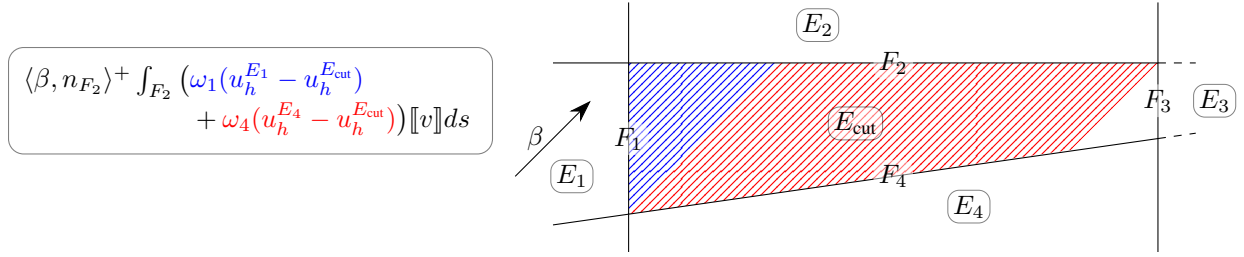


Fig. 2: Domain of dependence extension illustrated on a four-sided cut-cell: We introduce a direct mass transport from cells E_1 and E_4 into E_2 . The colored regions indicate the coupling between the faces, the corresponding parts of the stabilization term on F_2 are highlighted accordingly. From the graphic one can see that flow orientation and geometry play a central part in determining the right mass redistribution and the ω_i will have to be chosen accordingly. The face F_3 needs to be stabilized as well. Note that there should not be any coupling between between F_2 and F_3 as both are outflow faces.

3 Stabilization

To deal with small cut-cells, an additional term $J_h^0 = \sum_{E_{\text{cut}} \in \mathcal{I}} J_h^{0, E_{\text{cut}}}$ with \mathcal{I} being the set of small cut-cells that require stabilization is added to the space semi-discretization (we will comment on our choice in the numerical results below). This results in the following scheme: Find $u_h(t) \in \mathcal{V}_h^0(\mathcal{M}_h)$ such that

$$(\partial_t u_h(t), v_h)_{L^2(\Omega)} + a_h^{\text{upw}}(u_h, v_h) + J_h^0(u_h, v_h) + l_h(v_h) = 0 \quad \forall v_h \in \mathcal{V}_h^0(\mathcal{M}_h). \quad (4)$$

Let E_{cut} be a small cut-cell that requires stabilization. The idea behind $J_h^{0, E_{\text{cut}}}$ is the following: When the time step size is not chosen to respect the small size of E_{cut} , the domain of dependence of an outflow neighbor E of E_{cut} will extend beyond E_{cut} . We therefore extend the numerical DoD of E such that it receives information directly from the inflow neighbors of E_{cut} . The amount of mass passed directly between neighbors of E_{cut} is chosen such that the update on E_{cut} becomes stable.

To explain the main concept we consider the scalar linear transport equation $u_t + \nabla \cdot (\beta u) = 0$ with constant velocity $\beta = (\beta_1, \beta_2)^T \in \mathbb{R}^2$, i.e., we use $A = \beta_1, B = \beta_2$ in (1). Consider Fig. 2 where the domain of dependence of E_2 potentially reaches into E_1 and E_4 . In that case, for choosing the time step based on the size of background cells, mass (physically) is moved from E_1 and from E_4 to E_2 in a single time step and this coupling must be mimicked by the stabilization.

We introduce an extension operator $\mathcal{L}_{E'}^{\text{ext}}(u_h)(x) = u_h^{E'}(x)$ for $E' \in \mathcal{M}_h$ which acts on functions $u_h \in \mathcal{V}_h^0(\mathcal{M}_h)$ and corresponds to evaluating the (constant) polynomial of cell E' outside its original support. Using this operator, the following stabilization term was introduced in [4] for triangular cut-cells with single outflow face F_2 and single inflow face F_1 :

$$J_h^{0, E_{\text{cut}}}(u_h, v_h) = \eta_{E_{\text{cut}}} \int_{F_2} \langle \beta, n_{F_2} \rangle (\mathcal{L}_{E_1}^{\text{ext}}(u_h) - u_h^{E_{\text{cut}}}) \llbracket v_h \rrbracket ds. \quad (5)$$

This term introduces a direct coupling between E_1 and E_2 . The parameter $\eta_{E_{\text{cut}}} \in [0, 1]$ controls how much mass is transported via this coupling. In the case of exactly one inflow face F_1 and one outflow face F_2 (and one face with no-penetration b.c.), as considered in [4], this term suffices to ensure stability. Here, however, the cut-cell is allowed to have two inflow faces as illustrated in Fig. 2. Furthermore, these inflow faces will in general influence multiple neighbors of the cut-cell where the degree of influence depends on the geometry and flow direction. To handle this we propose the following extension of (5)

$$J_h^{0, E_{\text{cut}}}(u_h, v_h) = \eta_{E_{\text{cut}}} \sum_{F_j \in \mathcal{F}_h^{E_{\text{cut}}}} \int_{F_j} \sum_{F_i \in \mathcal{F}_h^{E_{\text{cut}}}} \omega_i \langle \beta, n_{F_j} \rangle^+ (\mathcal{L}_{E_i}^{\text{ext}}(u_h) - u_h^{E_{\text{cut}}}) \llbracket v_h \rrbracket ds. \quad (6)$$

Here the $\omega_i \in \mathbb{R}$ provide information about the flow distribution for incoming flow of the face F_i . Note that the extended solutions of all neighbor elements are evaluated on all faces, and $\omega_i = 0$ if F_i is not an inflow face. We provide a specific formula of how to choose these weights for triangular cut-cells below in section 3.2.

Going back to the system case we allow $\omega_i \in \mathbb{R}^{m \times m}$ and arrive at our final formulation

$$J_h^{0, E_{\text{cut}}}(u_h, v_h) = \eta_{E_{\text{cut}}} \sum_{F_j \in \mathcal{F}_h^{E_{\text{cut}}}} \int_{F_j} \sum_{F_i \in \mathcal{F}_h^{E_{\text{cut}}}} \langle \omega_i C_F^+ (\mathcal{L}_{E_i}^{\text{ext}}(u_h) - u_h^{E_{\text{cut}}}), \llbracket v_h \rrbracket \rangle ds. \quad (7)$$

Note that in defining $J^{0,E_{\text{cut}}}$ we assume that all normal vectors n_j for $F_j \in \mathcal{F}_h^{E_{\text{cut}}}$ correspond to *outward* normal vectors with respect to E_{cut} . In order to ensure consistency and stability the weights ω_i must fulfill

$$\sum_{F_i \in \mathcal{F}_h^{E_{\text{cut}}}} \omega_i = \text{Id}_{m \times m}, \quad (8)$$

$$\sum_{F_j \in \mathcal{F}_h^{E_{\text{cut}}}} \int_{F_j} \omega_i C_j^+ ds = - \int_{F_i} C_i^- ds \quad \forall F_i \in \mathcal{F}_h^{E_{\text{cut}}}. \quad (9)$$

Additionally we require that $\omega_i C_{F_j}^+$ is always symmetric and positive semi-definite. Equation (8) can be understood as an assurance that the overall amount of mass moved over a face by our stabilization is correct. For the scalar case, we require the ω_i to build a convex combination. Equation (9) means that a portion of the inflow is exactly redistributed over all outflow face candidates. This in particular prevents overshoots on small cut-cells for appropriate choices of $\eta_{E_{\text{cut}}}$.

3.1 L^2 -stability

Equipped with the aforementioned properties of our stabilization we can show L^2 -stability for the semi-discrete scheme in space. For brevity we consider homogeneous inflow boundary conditions and assume that exact and discrete solution vanish on the boundary, so that we can ignore any domain boundary terms and focus on the situation of cut-cells. For P^0 functions this means that they are zero in all boundary cells.

Theorem 3.1 *Consider (1) with homogeneous boundary conditions. Assume that the discrete solution $u_h(t)$ vanishes on the boundary $\partial\Omega$ for all $t \in (0, T)$. Let $u_h(t) \in \mathcal{V}_h^0(\mathcal{M}_h)$ be the solution to the semi-discrete problem (4). Then it holds*

$$\|u_h(t)\|_{L^2(\Omega)} \leq \|u_h(0)\|_{L^2(\Omega)} \quad \forall t \in (0, T).$$

Proof. We choose $v_h = u_h(t)$ in (4). Any boundary terms vanish as $\text{trace}(u_h(t)) = 0$ on $\partial\Omega$. This yields

$$(\partial_t u_h(t), u_h(t))_{L^2(\Omega)} + a_h^{\text{upw}}(u_h(t), u_h(t)) + J_h^0(u_h(t), u_h(t)) = 0.$$

By the fundamental theorem of calculus

$$\int_0^t (\partial_\tau u_h(\tau), u_h(\tau))_{L^2(\Omega)} d\tau = \int_0^t \frac{d}{d\tau} \frac{1}{2} \|u_h(\tau)\|_{L^2(\Omega)}^2 d\tau = \frac{1}{2} \|u_h(t)\|_{L^2(\Omega)}^2 - \frac{1}{2} \|u_h(0)\|_{L^2(\Omega)}^2.$$

To ease notation we will write $u = u_h(t)$ in the following. The goal now is to show that $a_h^{\text{upw}}(u, u) + J_h^0(u, u) \geq 0$. We first consider $a_h^{\text{upw}}(u, u)$, which expands into

$$\begin{aligned} a_h^{\text{upw}}(u, u) &= \sum_{F \in \mathcal{F}_h^{\text{int}}} \int_F \langle C_F \{u\}, [u] \rangle + \langle \frac{1}{2} |C_F| [u], [u] \rangle ds = \sum_{F \in \mathcal{F}_h^{\text{int}}} \int_F \langle C_F^+ u^{E_1} + C_F^- u^{E_2}, u^{E_1} - u^{E_2} \rangle ds \\ &= \sum_{F \in \mathcal{F}_h^{\text{int}}} \int_F \langle C_F^+ u^{E_1}, u^{E_1} \rangle - \langle C_F^+ u^{E_1}, u^{E_2} \rangle + \langle C_F^- u^{E_2}, u^{E_1} \rangle - \langle C_F^- u^{E_2}, u^{E_2} \rangle ds. \end{aligned}$$

Now we add zeros (in form of $\pm \frac{1}{2} \langle C_F^- u^{E_1}, u^{E_1} \rangle$ and $\pm \frac{1}{2} \langle C_F^+ u^{E_2}, u^{E_2} \rangle$) to get

$$\begin{aligned} &= \sum_{F \in \mathcal{F}_h^{\text{int}}} \int_F \frac{1}{2} \langle (C_F^+ - C_F^-) u^{E_1}, u^{E_1} \rangle + \frac{1}{2} \langle (C_F^+ + C_F^-) u^{E_1}, u^{E_1} \rangle - \langle C_F^+ u^{E_1}, u^{E_2} \rangle \\ &\quad + \langle C_F^- u^{E_2}, u^{E_1} \rangle + \frac{1}{2} \langle (C_F^+ - C_F^-) u^{E_2}, u^{E_2} \rangle - \frac{1}{2} \langle (C_F^+ + C_F^-) u^{E_2}, u^{E_2} \rangle ds \\ &= \sum_{F \in \mathcal{F}_h^{\text{int}}} \int_F \frac{1}{2} \langle |C_F| (u^{E_1} - u^{E_2}), u^{E_1} - u^{E_2} \rangle + \frac{1}{2} \langle C_F u^{E_1}, u^{E_1} \rangle - \frac{1}{2} \langle C_F u^{E_2}, u^{E_2} \rangle \\ &\quad - \frac{1}{2} \langle C_F u^{E_1}, u^{E_2} \rangle + \frac{1}{2} \langle C_F u^{E_2}, u^{E_1} \rangle ds. \end{aligned}$$

Due to the symmetry of C_F , the terms in the last line cancel each other. For the last two terms in the second to last line we use the divergence theorem. Since $u_h(t)$ is elementwise constant, on $E \in \mathcal{M}_h$ it holds that

$$0 = \int_E \nabla \cdot (\langle A u^E, u^E \rangle, \langle B u^E, u^E \rangle) dx = \sum_{F \in \mathcal{F}_h^{\text{int}} \cup \mathcal{F}_h^{\text{ext}}, F \cap \partial E \neq \emptyset} \int_F \langle C_F u^E, u^E \rangle ds,$$

and therefore, these terms vanish as well. Finally, due to $|C_F|$ being positive semi-definite, we obtain positivity of $a_h^{\text{upw}}(u, u)$:

$$a_h^{\text{upw}}(u, u) = \sum_{F \in \mathcal{F}_h^{\text{int}}} \int_F \frac{1}{2} \langle |C_F| (u^{E_1} - u^{E_2}), u^{E_1} - u^{E_2} \rangle ds \geq 0.$$

We now investigate J_h^0 . For a small cut-cell $E_{\text{cut}} \in \mathcal{I}$ we have due to (8)

$$\begin{aligned} J_h^{0, E_{\text{cut}}}(u, u) &= \eta_{E_{\text{cut}}} \sum_{F_j \in \mathcal{F}_h^{E_{\text{cut}}}} \int_{F_j} \langle (\sum_{F_i \in \mathcal{F}_h^{E_{\text{cut}}}} \omega_i C_{F_j}^+ u^{E_i}) - C_{F_j}^+ u^{E_{\text{cut}}}, u^{E_{\text{cut}}} - u^{E_j} \rangle ds \\ &= \eta_{E_{\text{cut}}} \sum_{F_j \in \mathcal{F}_h^{E_{\text{cut}}}} \int_{F_j} \langle \sum_{F_i \in \mathcal{F}_h^{E_{\text{cut}}}} \omega_i C_{F_j}^+ u^{E_i}, u^{E_{\text{cut}}} \rangle - \langle \sum_{F_i \in \mathcal{F}_h^{E_{\text{cut}}}} \omega_i C_{F_j}^+ u^{E_i}, u^{E_j} \rangle \\ &\quad - \langle C_{F_j}^+ u^{E_{\text{cut}}}, u^{E_{\text{cut}}} \rangle + \langle C_{F_j}^+ u^{E_{\text{cut}}}, u^{E_j} \rangle ds. \end{aligned}$$

Adding again zeros (in form of $\pm \langle \sum_{F_i \in \mathcal{F}_h^{E_{\text{cut}}}} \omega_i C_{F_j}^+ u^{E_i}, u^{E_i} \rangle$ and $\pm \langle C_{F_j}^+ u^{E_j}, u^{E_j} \rangle$) and reordering gives

$$\begin{aligned} &= -\frac{1}{2} \eta_{E_{\text{cut}}} \sum_{F_j \in \mathcal{F}_h^{E_{\text{cut}}}} \int_{F_j} \langle C_{F_j}^+ u^{E_{\text{cut}}}, u^{E_{\text{cut}}} \rangle - 2 \langle C_{F_j}^+ u^{E_{\text{cut}}}, u^{E_j} \rangle + \langle C_{F_j}^+ u^{E_j}, u^{E_j} \rangle \\ &\quad + \langle \sum_{F_i \in \mathcal{F}_h^{E_{\text{cut}}}} \omega_i C_{F_j}^+ u^{E_i}, u^{E_i} \rangle - 2 \langle \sum_{F_i \in \mathcal{F}_h^{E_{\text{cut}}}} \omega_i C_{F_j}^+ u^{E_i}, u^{E_{\text{cut}}} \rangle + \langle C_{F_j}^+ u^{E_{\text{cut}}}, u^{E_{\text{cut}}} \rangle \\ &\quad - \langle \sum_{F_i \in \mathcal{F}_h^{E_{\text{cut}}}} \omega_i C_{F_j}^+ u^{E_i}, u^{E_i} \rangle + 2 \langle \sum_{F_i \in \mathcal{F}_h^{E_{\text{cut}}}} \omega_i C_{F_j}^+ u^{E_i}, u^{E_j} \rangle - \langle C_{F_j}^+ u^{E_j}, u^{E_j} \rangle ds \\ &= -\frac{1}{2} \eta_{E_{\text{cut}}} \sum_{F_j \in \mathcal{F}_h^{E_{\text{cut}}}} \int_{F_j} \langle C_{F_j}^+ (u^{E_{\text{cut}}} - u^{E_j}), u^{E_{\text{cut}}} - u^{E_j} \rangle \\ &\quad + \sum_{F_i \in \mathcal{F}_h^{E_{\text{cut}}}} \langle \omega_i C_{F_j}^+ (u^{E_i} - u^{E_{\text{cut}}}), u^{E_i} - u^{E_{\text{cut}}} \rangle \quad (C_{F_j}^+, \omega_i C_{F_j}^+ \text{ symm. and (8)}) \\ &\quad - \sum_{F_i \in \mathcal{F}_h^{E_{\text{cut}}}} \langle \omega_i C_{F_j}^+ (u^{E_i} - u^{E_j}), u^{E_i} - u^{E_j} \rangle ds \\ &\stackrel{(9)}{=} -\frac{1}{2} \eta_{E_{\text{cut}}} \sum_{F_j \in \mathcal{F}_h^{E_{\text{cut}}}} \int_{F_j} \langle |C_{F_j}| (u^{E_{\text{cut}}} - u^{E_j}), u^{E_{\text{cut}}} - u^{E_j} \rangle \\ &\quad - \sum_{F_i \in \mathcal{F}_h^{E_{\text{cut}}}} \langle \omega_i C_{F_j}^+ (u^{E_i} - u^{E_j}), u^{E_i} - u^{E_j} \rangle ds. \end{aligned}$$

Since $\eta_{E_{\text{cut}}} \in [0, 1]$ the first term inside the sum can be compensated with terms from a_h^{upw} . The second term is always non-negative since $\omega_i C_{F_j}^+$ is always positive semi-definite. Note that the second term corresponds to dissipation introduced by an extended jump. This concludes the proof. \square

3.2 Choice of parameters

To perform actual computations we need to select concrete ω_i in (7) that fulfill properties (8) and (9). For the situation of linear simultaneously diagonalizable hyperbolic systems and triangular cut-cells we suggest $\omega_i = |F_i| C_{F_i}^- (\sum_{F_k \in \mathcal{F}_h^{E_{\text{cut}}}} |F_k| C_{F_k}^-)^{-1}$ for each $F_i \in \mathcal{F}_h^{E_{\text{cut}}}$. For linear advection, this would result in $\omega_i = 0$ for an outflow edge F_i and ω_i corresponding to some sort of weighted proportion of the total inflow for an inflow edge F_i . We also need to set $\eta_{E_{\text{cut}}}$ for $E_{\text{cut}} \in \mathcal{I}$. A stable but not necessarily optimal choice is $\eta_{E_{\text{cut}}} = \|\sum_{F \in \mathcal{F}_h^{E_{\text{cut}}}} \int_F \Lambda_F^- ds\|_\infty$.

4 Numerical results

For the numerical tests we select angles $\gamma, \theta, \rho_1, \rho_2 \in [0, 2\pi)$ where γ is the angle of the cut, see Fig. 1, and set

$$\Lambda_1 = \begin{pmatrix} \cos(\rho_1) & 0 \\ 0 & \cos(\rho_2) \end{pmatrix}, \quad \Lambda_2 = \begin{pmatrix} \sin(\rho_1) & 0 \\ 0 & \sin(\rho_2) \end{pmatrix}, \quad O = \begin{pmatrix} \cos(\theta) & -\sin(\theta) \\ \sin(\theta) & \cos(\theta) \end{pmatrix}.$$

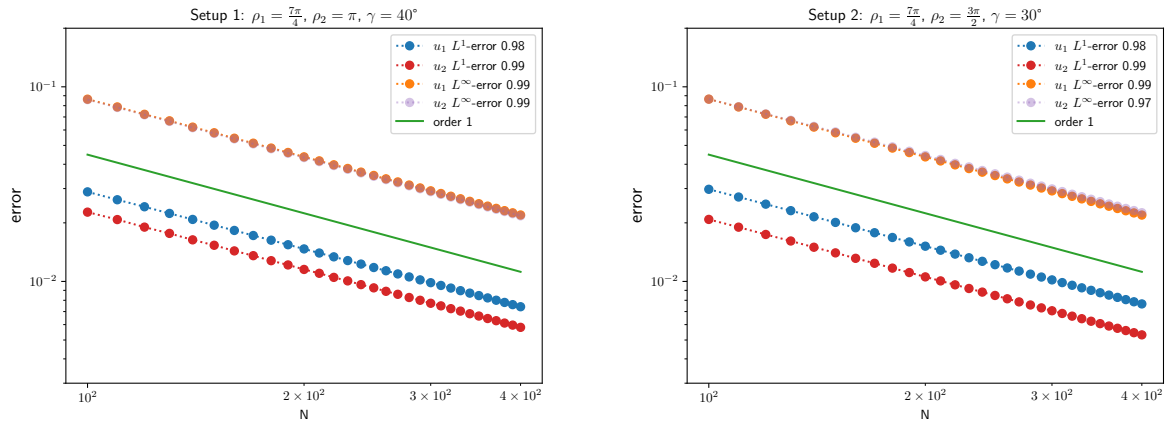


Fig. 3: Plots of the error, measured in the L^1 - (blue, red) and L^∞ -norm (orange, transparent purple). Left plot has values $\rho_1 = \frac{7\pi}{4}$, $\rho_2 = \pi$ and $\gamma = 40^\circ$, right plot has $\rho_1 = \frac{7\pi}{4}$, $\rho_2 = \frac{3\pi}{2}$ and $\gamma = 30^\circ$. In all cases we have chosen $\theta = \frac{4\pi}{3}$. The green line is for reference.

Then our system matrices will be given by $A = O\Lambda_1 O^T$ and $B = O\Lambda_2 O^T$.

The cut starts at $(x_0, 0) = (0.2001, 0)$. As initial conditions we choose $u_0(x) = O \begin{pmatrix} \sin(2\pi(x_1 \cos(\rho_1) + x_2 \sin(\rho_1))) \\ \cos(2\pi(x_1 \cos(\rho_2) + x_2 \sin(\rho_2))) \end{pmatrix}$. Boundary conditions are given by the exact solution. Let N denote the number of background cells in either coordinate direction. We compute the time step size via $\Delta t = 0.4 \frac{h}{\max_{n \in \mathbb{S}^1} \|n_1 \Lambda_1 + n_2 \Lambda_2\|_\infty}$, where $h = \frac{1}{N}$. The factor of 0.4 allows that bigger cut-cells do not need to be stabilized. We then choose $\mathcal{I} = \{E \in \mathcal{M}_h \mid \frac{|E|}{h^2} < 0.4\}$ as the set of stabilized cut-cells. The final time of our simulation is $T = 0.5$.

Our implementation is based on the DUNE framework (see [2], [1]), in particular the dune-udg (see [3], [5]) and dune-pdelab modules. The local subtriangulations for the cut-cells are computed by the TPMC library (see [6]).

Fig. 3 shows convergence plots for two particular setups. Note that the flow directions have been chosen to *not* be parallel to the ramp angle γ . We observe the expected order of convergence for a first order scheme in both the L^1 - and the L^∞ -norm. In addition, all numerically computed solution values, including those on small cut-cells, stayed within the bounds of the initial state during the simulation, confirming the added stability of the DoD stabilization.

5 Discussion and Outlook

We have extended the DoD stabilization to cut-cells with multiple inflow/outflow faces for the case of component-wise and piecewise constant trial and test functions and linear, simultaneously diagonalizable systems in two dimensions. We have proven L^2 -stability for the semi-discrete setting. Numerically we observe full first-order convergence in different numerical tests and no over/undershoot on cut-cells. In future work, we plan to extend our method to more general systems, e.g., the acoustics and Euler equations. An extension of the presented formulation to higher-order approximations is ongoing research.

Acknowledgements This work has been partially funded by the Deutsche Forschungsgemeinschaft (DFG, German Research Foundation) as project 439956613 under contract numbers EN 1042/5-1 and MA 7773/4-1/2.

References

- [1] P. Bastian, M. Blatt, A. Dedner, C. Engwer, R. Klöforn, R. Kornhuber, M. Ohlberger, and O. Sander, *Computing*, **82**, 121-138 (2008)
- [2] P. Bastian, M. Blatt, A. Dedner, C. Engwer, R. Klöforn, M. Ohlberger, and O. Sander, *Computing*, **82**, 103-119 (2008)
- [3] P. Bastian and C. Engwer, *Int. Jour. for Num. Meth. in Eng.*, **79**, **12**, 1557-1576 (2009)
- [4] C. Engwer, S. May, A. Nüßing, and F. Streitbürger, *SIAM J. Sci. Comput.* **42**, **6**, A3677-A3703 (2020).
- [5] C. Engwer and F. Heimann, *Proceedings of the DUNE user meeting, Stuttgart, Germany, Advances in DUNE (Springer Berlin, Heidelberg, 2012)* pp. 89-100
- [6] C. Engwer and A. Nüßing, *ACM Trans. on Math. Soft.*, **44**, **2**, Art. No. 14 (2018)
- [7] P. Fu and G. Kreiss, *SIAM J. Sci. Comput.*, **43**, **4**, A2404-A2424, 2021.
- [8] A. Giuliani, *SIAM J. Sci. Comput.* **44**, **1**, A389-A415 (2022)
- [9] S. May, F. Streitbürger, *Appl. Math. Comput.* **419**, Art. 126854 (2022).
- [10] S. Schoeder, S. Sticko, G. Kreiss and M. Kronbichler, *Int. J. Numer. Meth. Engrg.* **121**, **13**, 2979-3003 (2020)
- [11] F. Streitbürger, G. Birke, C. Engwer, and S. May, *Spectral and High Order Methods for Partial Differential Equations ICOSAHOM 2020+1.*, **137** (Springer International Publishing, 2023).